Monatsh Chem (2017) 148:209–216
DOI 10.1007/s00706-016-1777-8

ORIGINAL PAPER

Solvothermal syntheses, crystal structures, and properties of new lanthanide compounds based on tetraselenidoantimonate and tetraethylenepentamine mixed ligands

Peipei Sun[1] · Shuzhen Liu[1] · Jingyu Han[1] · Yali Shen[1] · Yun Liu[1] · Chunying Tang[1] · Dingxian Jia[1]

Received: 25 February 2016 / Accepted: 10 May 2016 / Published online: 20 June 2016

Abstract New lanthanide(III) compounds $[[Ln(tepa)(Cl)]-[Ln(tepa)(OH)]_2(SbSe_4)_2]_n$ (Ln=Sm, Eu), $[H_2tepa][[Ln(tepa)-(SbSe_4)]_2(OH)_2]$ (Ln=Eu, Gd, Ho) (tepa=tetraethylenepentamine) were prepared by solvothermal methods. Acting as a bidentate μ-1κ:2κ-$SbSe_4$ bridging ligand, the $[SbSe_4]^{3-}$ unit interconnects $[[Ln(tepa)]_2(OH)_2]^{4+}$ and $[Ln(tepa)Cl]^{2+}$ (Ln=Sm, Eu) ions to form one-dimensional coordination polymers $[[Ln(tepa)(Cl)][Ln(tepa)(OH)]_2(SbSe_4)_2]_n$. The $[SbSe_4]^{3-}$ unit acts as monodentate ligand to Ln(III) centers in $[H_2tepa][[Ln(tepa)(SbSe_4)]_2(OH)_2]$. The different coordination modes of the $[SbSe_4]^{3-}$ units in $[[Ln(tepa)(Cl)][Ln-(tepa)(OH)]_2(SbSe_4)_2]_n$ and $[H_2tepa][[Ln(tepa)(SbSe_4)]_2-(OH)_2]$ are attributed to the size of Ln^{3+} ions. The bidentate μ-1κ:2κ-$SbSe_4$ bridging ligand in $[[Ln(tepa)(Cl)][Ln(tepa)-(OH)]_2(SbSe_4)_2]_n$ is observed in the lanthanide complexes of tetraselenidoantimonate ligands for the first time. All compounds exhibit steep band gaps between 2.04 and 2.31 eV at room temperature.

Graphical abstract

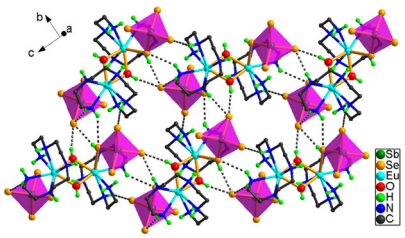

Keywords Chalcogenides · Ligands · Coordination mode · Single crystal X-ray structure determination · UV/vis spectroscopy

Introduction

Chalcogenides of group 15 metals have drawn increasing interest due to their structural diversity, and potential applications in many areas such as fast-ion conductivity, semiconductivity, photo-catalyst, nonlinear optical material [1–8]. In the past decade, solvothermal synthesis in a coordinative amine media has proven to be a useful approach to the ternary chalcogenidoantimonates containing transition metal (TM) components [9–13], since the cobalt thioantimonate $[Co(en)_3]CoSb_4S_8$ was prepared by the reaction of $CoBr_2$ and Na_3SbS_3 in ethylenediamine (en) at 130 °C [14]. The coordinative amine acts as not only the reaction solvent but also the ligand to TM^{n+} ion in the solvothermal reaction. Composition and structure of the coordinative amine show substantial influence on the combination between TM centers and chalcogenidoantimonate anions. A large number of chalcogenidoantimonates containing free d-block TM complexes

Electronic supplementary material The online version of this article (doi:10.1007/s00706-016-1777-8) contains supplementary material, which is available to authorized users.

✉ Dingxian Jia
jiadingxian@suda.edu.cn

[1] College of Chemistry, Chemical Engineering and Materials Science, Soochow University, Suzhou 215123, People's Republic of China

have been prepared in bidentate en and tridentate dien (dien=diethylenetriamine) solvents because of the formation of coordination-saturated octahedra $[TM(en)_3]^{n+}$ and $[TM(dien)_2]^{n+}$ complexes ions [15–23]. Only a few ternary chalcogenidoantimonates integrated with TM were prepared in en and dien, and the examples include $Cr(en)_2SbS_3$ [24], $[Mn_2(en)_2(Sb_2S_5)]$ [25], $[Mn_2(dien)(Sb_2S_5)]$ [26], $[Mn_4(en)_9(SbSe_4)_4]^{4-}$ [27], $[Mn_2(SbSe_4)_2(en)_4(H_2O)]^{2-}$ [28], and $(dienH_3)[(dienH)MnSb_8S_{15}]\,H_2O$ [29]. On the other hand, the TM^{n+} ions are easily incorporated with chalcogenidoantimonates using tetradentate tris(2-aminoethyl)amine (tren) and pentadentate tetraethylenepentamine (tepa) as the coligands to the TM^{n+} centers. The tren or tepa coligands leave one or two coordination sites free for the TM^{n+} ions to form TM–S or TM–Se bond with the chalcogenidoantimonate anions. As a result, ternary TM-chalcogenidoantimonates were obtained [30–38].

In comparison to the ternary TM-chalcogenidoantimonates, which are constructed from TM^{n+} ions and chalcogenidoantimonate anions via TM–S or TM–Se bond, the weak interactions between lanthanide (Ln) ions and chalcogenidoantimonate anions make the synthesis of ternary Ln-chalcogenidoantimonates a challenging task. However, our work has demonstrated that the chalcogenidoantimonate anions $[SbS_4]^{3-}$ and $[SbSe_4]^{3-}$ can coordinate to Ln(III) centers using coordinative amines as co-ligands, and a number of Ln-chalcogenidoantimonates have been solvothermally prepared in en, dien, and trien solvents [39–44]. Unlike the TM^{n+} metals which exhibit restricted stereochemistry in coordination complexes, the Ln^{3+} ions are characterized by variable geometries due to their higher coordination numbers [45], which theoretically provides the Ln^{3+} ions with different structural features from the TM^{n+} ions in the combination with chalcogenidoantimonate anionic ligands in the presence of the same ethylene polyamines. The Ln^{3+} ions can form unsaturated complex units with en and dien ligands, as well as with tetradentate trien ligand or en+dien, and en+trien mixed ligands. The $[SbS_4]^{3-}$ or $[SbSe_4]^{3-}$ anions complete the unsaturated coordination sites of Ln^{3+} centers via Ln–S or Ln–Se bond formation. Furthermore, the $[SbS_4]^{3-}$ or $[SbSe_4]^{3-}$ anions can be tuned to coordinate to Ln(III) centers in mono-SbQ_4, $1\kappa^2$-SbQ_4 and μ-$1\kappa,2\kappa^2$-SbQ_4 (Q=S, Se) coordination modes using ethylene polyamines en, dien and trien as the co-ligands [39–44]. It is important to systematically investigated the synergistic coordination effects of SbQ_4 and polyamino ligands on the Ln(III) centers in the preparation of new Ln-containing chalcogenidometalates. By using identical Ln(III) metals and SbQ_4 tetrahedra as building blocks, structural diversities could be obtained by virtue of ethylene polyamino ligands with different denticities. The solvothermal syntheses of lanthanide chalcogenidoantimonates in polyamines with higher denticities remain less explored, although a few lanthanide chalcogenidoantimonates were prepared in pentadentate tepa [46–48] and hexadentate pentaethylenehexamine (peha) [49]. Now, the $LnCl_3$ (Ln_2O_3)/Sb/Se (Ln=Sm, Eu, Gd, Ho) system was investigated in tepa, and new members of the Ln–Sb–Se compound family $[[Ln(tepa)(Cl)][Ln(tepa)(OH)]_2(SbSe_4)_2]_n$ (Ln=Sm (**1a**), Eu (**1b**)), and $[H_2tepa][[Ln(tepa)(SbSe_4)]_2(OH)_2]$ (Ln=Eu (**2a**), Gd (**2b**), Ho (**2c**)) were prepared using solvothermal methods. The influences of tepa coligands and ionic size of the Ln(III) ions on coordination modes of the tetraselenidoantimonate anion $[SbSe_4]^{3-}$are discussed.

Results and discussion

Syntheses

Solvothermal reactions of Sb, Se with $SmCl_3$ ($EuCl_3$) in tepa at 190 °C for 7 days produced polymeric lanthanide(III) compounds $[[Ln(tepa)(Cl)][Ln(tepa)(OH)]_2(SbSe_4)_2]_n$ (Ln=Sm (**1a**), Eu (**1b**)). The reactions with Ln_2O_3 as starting material under the same conditions afforded complexes $[H_2tepa][[Ln(tepa)(SbSe_4)]_2(OH)_2]$ (Ln=Eu (**2a**), Gd (**2b**), Ho (**2c**)). Polyamine tepa not only acts as solvent of the solvothermal reaction, but also takes part in the coordination to Ln(III) centers as coligand. Recently, Zhou reported the complexes $[Ln_2(tepa)_2(\mu\text{-}OH)_2Cl_2][[Ln(tepa)]_2(\mu\text{-}OH)_2(SbSe_4)_2]$ (Ln=Sm, Gd), which were prepared by the reaction at 170 °C for 6 days in tepa using $LnCl_3$ as starting materials [48]. Comparing the Sm and Gd complexes in tepa, reaction conditions and Cl^- ion influence the solvothermal syntheses of the Sb/Se system in tepa.

Crystal Structures of 1a and 1b

Compounds **1a** and **1b** crystallize in the monoclinic space group *C*2/c with four units in the unit cell. They are isostructural and consist of one-dimensional (1-D) coordination polymers constructed by $[[Ln(tepa)]_2(OH)_2]^{4+}$, $[Ln(tepa)Cl]^{2+}$, and $[SbSe_4]^{3-}$ fragments. The crystal structure of **1a** is illustrated in Figs. 1 and 2. As shown in Fig. 1, $Sm(1)^{3+}$ ion is coordinated by a pentadentate tepa forming a $[Sm(tepa)]^{3+}$ unit. Two $[Sm(tepa)]^{3+}$ units are joined by two μ-OH bridging ligands to form the binuclear $[[Sm(tepa)]_2(OH)_2]^{4+}$ complex fragment. The separation of Sm(1)···Sm(1A) in the binuclear unit is 3.8100(7) Å, which is comparable to that observed in $[[Sm(en)]_3(OH)_2]^{4+}$ [(Sm···Sm = 3.844(2) Å)] [50]. $Sm(2)^{3+}$ ion is coordinated by a tepa and a Cl^-ligand to form the $[Sm(tepa)Cl]^{2+}$ fragment. The $Sm(2)^{3+}$ and Cl^- ions are disordered and the occupancies of both ions being refined as 50 % each. The

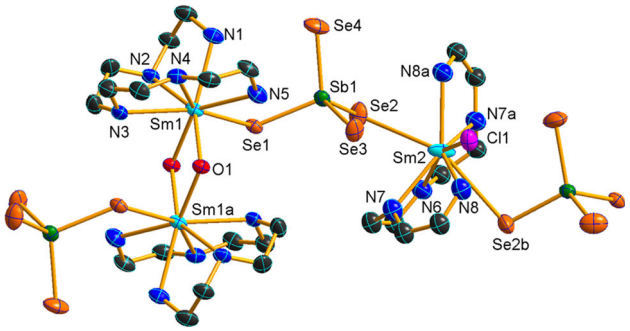

Fig. 1 Molecular structure of **1a**, showing atom labels. Hydrogen atoms are omitted for clarity

Sb^{5+} ion binds four Se^{2-} anions with distances in the range of 2.4427(12)–2.4821(10) Å, generating a tetrahedral $[SbSe_4]^{3-}$ unit with Se–Sb–Se angles in the range of 105.62(4)°–112.01(5)° (Table 1). The bond lengths and angles are consistent with the corresponding values observed in the selenidoantimonates containing $[SbSe_4]^{3-}$ unit [41–44, 48]. Acting as a bidentate μ-1κ:2κ-$SbSe_4$ bridging ligand, the $[SbSe_4]^{3-}$ (A) unit interconnects the $[[Sm(tepa)]_2(OH)_2]^{4+}$ (B) and $[Sm(tepa)Cl]^{2+}$ (C) fragments to a neutral coordination polymer $[[Sm(tepa)(Cl)][Sm(tepa)(OH)]_2(SbSe_4)_2]_n$ (Fig. 2), in which three fragments are repeated in the order of [–ABACABAC–]. Both $Sm(1)^{3+}$ and $Sm(2)^{3+}$ ions are in an eightfold coordination environment, forming a SmN_5O_2Se and a SmN_5Se_2Cl polyhedra, respectively (Fig. S1). The bond lengths Sm–N [(2.576(6)–2.638(18) Å)], Sm–Se [(3.0162(9)–3.334(3) Å)], Sm–O [(2.295(5) and 2.328(5) Å)] and Sm–Cl [(3.02(3) Å)] are in the range of those observed in literature [41–44, 48].

In **1a**, the 1-D polymeric chains $[[Sm(tepa)(Cl)][Sm(tepa)(OH)]_2(SbSe_4)_2]_n$ run parallel to each other. The chains are interconnected to a layer parallel to the (111) plane of the unit cell via weak N–H···Se hydrogen bonds

Table 1 Selected bond lengths (Å) and angles (°) for **1a** and **1b**

	1a (Ln=Sm)	**1b** (Ln=Eu)
Sb–Se	2.4427 (12)–2.4821 (10)	2.4419 (13)–2.4832 (10)
Ln–Se	3.0162 (9)–3.334 (3)	3.0152 (10)–3.453 (4)
Ln–O	2.295 (5), 2.328 (5)	2.292 (5), 2.334 (6)
Ln–N	2.576 (6)–2.606 (6)	2.558 (8)–2.603 (7)
Ln–Cl	3.05 (3)	3.16 (3)
Se–Sb–Se	105.62 (4)–112.01 (5)	105.21 (5)–111.76 (6)
Sb–Se–Ln	92.97 (12)–116.92 (3)	94.73 (13)–103.50 (8)
O–Ln–O	68.98 (19)	69.2 (2)
O–Ln–N	76.2 (2)–150.8 (2)	76.6 (2)–151.0 (2)
N–Ln–N	61.4 (4)–151.8 (9)	59.2 (5)–152.5 (9)
O–Ln–Se	72.83 (13), 100.17 (14)	72.68 (14), 100.48 (15)
N–Ln–Se	67.82 (12)–149.79 (16)	65.49 (12)–149.60 (18)

[N···Se: 3.529(7)–3.648(8) Å; N–H···Se: 138.4°–176.2°] (Fig. 2, Table S6). The N···Se separations and N–H···Se angles are in agreement with reported values observed in Ln tetraselenidoantimonate containing amino coligands [41–44, 48]. The layers are further connected through interlayer N–H···Se interactions to form a 3-D H-bonding network (Fig. S2). Orientations of the neighboring $[[Sm(tepa)(Cl)][Sm(tepa)(OH)]_2(SbSe_4)_2]_n$ chains alternate in the same layer.

Crystal structures of 2a–2c

Compounds **2a**–**2c** are isostructural. They are composed of a $[[Ln(tepa)(SbSe_4)]_2(OH)_2]^{2-}$ (Ln=Eu, Gd, Ho) anion and a protonated $[H_2tepa]^{2+}$ cation. The molecular structure of **2a** is depicted in Fig. 3. The Eu^{3+} ion is coordinated by a pentadentate tepa ligand and a monodentate $[SbSe_4]^{3-}$ ligand forming a $[Eu(tepa)(SbSe_4)]$ unit. Two [Eu(tepa)-

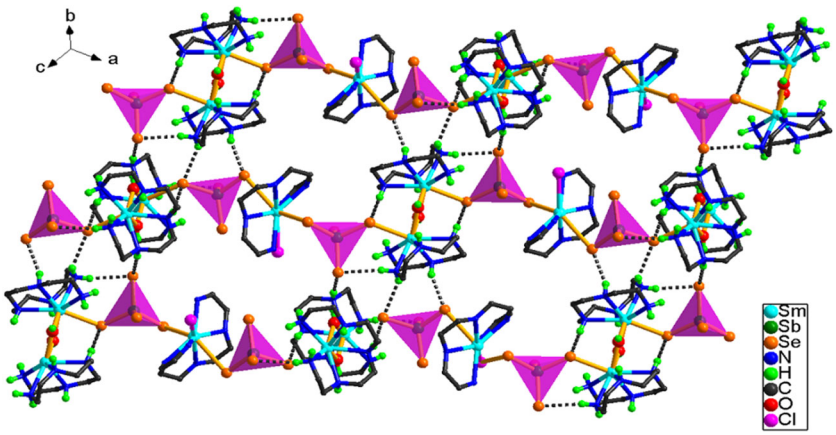

Fig. 2 A view of the layer constructed by $[[Sm(tepa)(Cl)][Sm(tepa)(OH)]_2(SbSe_4)_2]_n$ chains via N–H···Se interactions (shown in *dashed lines*) in **1a**. Hydrogen atoms of CH_2 groups are omitted for clarity. The $SbSe_4$ unit is shown in *purple* tetrahedron (color figure online)

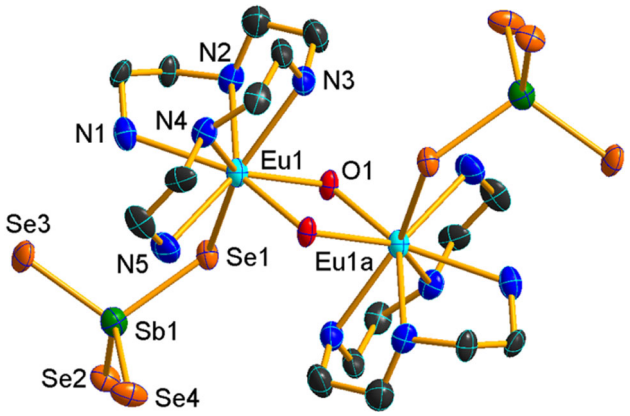

Fig. 3 Molecular structure of the $[[Eu(tepa)(SbSe_4)]_2(OH)_2]^{2-}$ anion in **2a**, showing atom labels. Hydrogen atoms are omitted for clarity

$(SbSe_4)]$ units are linked by two μ-OH bridging groups to generate a binuclear $[[Eu(tepa)(SbSe_4)]_2(OH)_2]^{2-}$ complex anion (Fig. 3). The Eu^{3+} ion is coordinated by five N, two O, and one Se atoms in a distorted bicapped trigonal prismatic environment (Fig. S3). The bond lengths and angles of the $[[Eu(tepa)(SbSe_4)]_2(OH)_2]^{2-}$ anion are similar to those of **1b** (Tables 1, 2). The Ln–Se, Ln–O, and Ln–N bond lengths decrease from Eu to Ho in compounds **2a**–**2c**, due to lanthanide contraction (Table 2). The Se(1), Se(2), and Se(3) atoms have contacts with amino groups NH and NH_2 of neighboring $[[Eu(tepa)(SbSe_4)]_2(OH)_2]^{2-}$ units with N···Se separations varying between 3.551(12) and 3.725(11) Å, and N–H···Se angles varying in 142.5°–176.1° (Table S6). In addition, Se(1) atom also interacts with a neighbor hydroxyl group OH^- (O···Se = 3.494(8) Å, O–H···Se = 168.2°). Each $[[Eu(tepa)(SbSe_4)]_2(OH)_2]^{2-}$ unit contact four neighbors with N–H···Se and O–H···Se hydrogen bonds. As a result, the $[[Eu(tepa)(SbSe_4)]_2(OH)_2]^{2-}$ units are connected to a layer perpendicular to the *a* axis (Fig. 4a). The protonated $[H_2tepa]^{2+}$ cations are

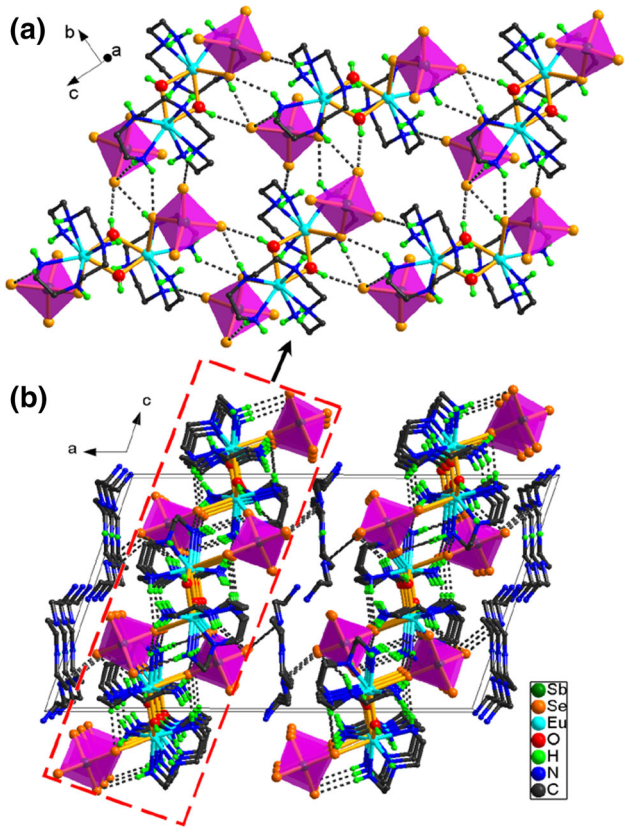

Fig. 4 **a** A view of the layer constructed by $[[Eu(tepa)(SbSe_4)]_2(OH)_2]^{2-}$ moieties via O–H···Se and N–H···Se interactions (shown in *dashed lines*) in **2a**. **b** Crystal packing of **2a** viewed along the *b* axis. The $SbSe_4$ unit is shown in *purple* tetrahedron. Hydrogen atoms of CH_2 groups are omitted for clarity (color figure online)

located between the layers, and interact with the layer via N–H···Se hydrogen bonds (Fig. 4b).

In our previous studies on solvothermal syntheses of Ln(III) selenidoantimonates, we have found that the tetraselenidoantimonate $[SbSe_4]^{3-}$ anion can be tuned to

Table 2 Selected bond lengths (Å) and angles (°) for **2a**–**2c**

	2a (Ln=Eu)	**2b** (Ln=Gd)	**2c** (Ln=Ho)
Sb–Se	2.4427 (19)–2.4874 (16)	2.4487 (17)–2.4847 (15)	2.4470 (18)–2.4866 (17)
Ln–Se	3.0426 (15)	3.0238 (14)	3.0035 (16)
Ln–O	2.289 (8), 2.331 (8)	2.290 (8), 2.319 (7)	2.240 (8), 2.282 (8)
Ln–N	2.564 (10)–2.596 (10)	2.568 (10)–2.595 (10)	2.509 (12)–2.543 (11)
Se–Sb–Se	106.77 (6)–111.26 (7)	106.49 (5)–111.36 (7)	106.79 (6)–111.41 (7)
Sb–Se–Ln	117.14 (5)	117.67 (5)	118.53 (5)
O–Ln–Se	72.98 (19), 102.1 (2)	72.6 (2), 102.0 (2)	72.4 (2), 102.0 (2)
O–Ln–O	69.0 (3)	69.0 (3)	68.0 (3)
O–Ln–N	76.9 (3)–151.2(3)	77.0 (3)–150.9 (3)	76.9 (3)–150.7 (3)
N–Ln–N	66.2 (4)–140.8(4)	66.8 (3)–141.2 (4)	67.0 (4)–141.0 (4)
Se–Ln–N	82.1 (2)–147.9 (2)	81.8 (3)–143.5 (2)	81.5 (3)–148.5 (3)

coordinate to Ln(III) centers with varying coordination modes using ethylene polyamino coligands like en, dien, trien or their mixtures [41–44]. Being multidentate chelating ligands with N-donor atoms, ethylene polyamines are prone to chelating the Ln(III) ions, but usually leave one or more coordination sites free due to steric hindrance of the polyamines. The numbers of left coordination sites are related to the structure of ethylene polyamine and the size of Ln(III) ion. The $[SbSe_4]^{3-}$anion coordinates to the remaining coordination sites and completes the coordination environment around the Ln(III) ions. As a result, Ln(III)–$SbSe_4$ complexes with different coordination modes of the $[SbSe_4]^{3-}$ ligand are obtained. Detailed investigation of the Ln/Sb/Se system in en, for instance, gave two types of Ln(III) compounds $[Ln(en)_4(SbSe_4)]$ (Ln=La, Pr, Nd) and $[Ln(en)_4]SbSe_4{\cdot}0.5en$ (Ln=Sm, Eu, Gd) [41–43].The former contains a 9-coordinated Ln(III) ion with a N_8 + Se donor set and a monodentate $[SbSe_4]^{3-}$ ligand, while the later contains a 8-coordinated Ln(III) ion with N_8 donor set and a free $[SbSe_4]^{3-}$anion. A similar investigation in dien solvent also produced two types of Ln(III) compounds $[Ln(dien)_2(\mu\text{-}1\kappa^2{:}2\kappa\text{-}SbSe_4)]_n$ (Ln=La, Pr, Nd) and $[Ln(dien)_2(1\kappa^2\text{-}SbSe_4)]$ (Ln = Sm, Eu, Gd), which contain a 9-coordinated Ln(III) ion with a N_6 + Se_3 donor set and a 8-coordinated Ln(III) ion with a N_6 + Se_2 donor set, respectively [41, 42]. Different coordination modes of the $[SbSe_4]^{3-}$ anion across the lanthanide series are also observed in en + dien and en + trien mixtures [41, 44]. It is worthy to note that La^{3+}–Nd^{3+} ions always possess coordination number of nine, while the ions beyond Nd^{3+} possess coordination number of eight [41–44]. Now, the solvothermal syntheses in tepa solvent gave two types of Ln(III)–$SbSe_4$ compounds **1a**, **1b**, and **2a**–**2c**, in which μ-1κ:2κ-$SbSe_4$ and mono-$SbSe_4$ ligands were obtained. The bidentate bridging μ-1κ:2κ-$SbSe_4$ ligand in **1a**, **1b** features a new coordination mode observed in Ln/Sb/Se systems. It is notable that **2a** is the first Ln(III) selenidoantimonate containing a 9-coordinated Sm(III) ion with a N_6 + Se_3 donor set. In summary, the coordination mode of $[SbSe_4]^{3-}$ is a result of synergetic effect of the structure of ethylene polyamine and the size of Ln(III) ion.

Solid state absorption spectra

Solid state optical diffuse reflection spectra of **1a**–**2c** were measured on powder samples at room temperature. The absorption data were calculated from the reflectance using the Kubelka–Munk function [51]. The obtained spectra of the complexes show well-defined abrupt absorption edges from which the band gaps can be estimated at 2.07, 2.18, 2.24, 2.22, and 2.31 eV for **1a**, **1b**, **2a**–**2c,** respectively (Figs. 5, 6), showing that the title compounds exhibit

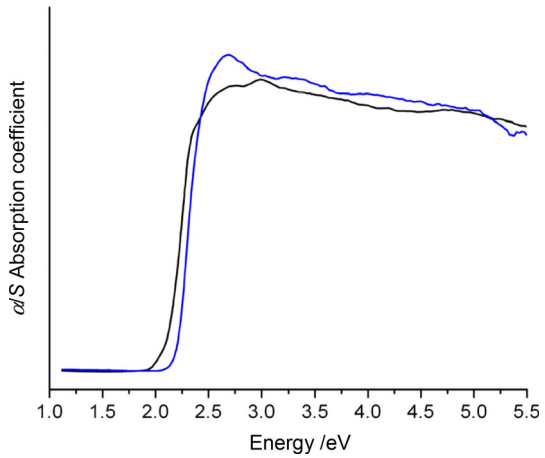

Fig. 5 Solid state optical absorption spectra of compounds **1a** (*black*), **1b** (*blue*) (color figure online)

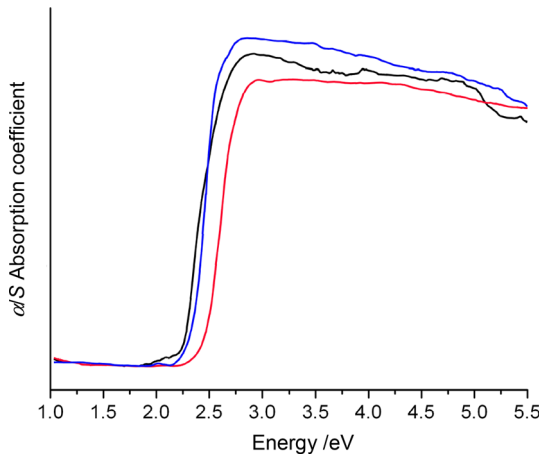

Fig. 6 Solid state optical absorption spectra of compounds **2a** (*blue*), **2b** (*black*), and **2c** (*red*) (color figure online)

potential semi-conducting properties. The band gaps (E_g) are similar to those of $[Ln(dien)_2(1\kappa^2\text{-}SbSe_4)]$ (Ln=Sm, Eu, Gd) (E_g: 2.19–2.28 eV) [41, 42], but are much higher than those of the layered copper selenidoantimonate compounds $Cs_2Cu_2Sb_2Se_5$ (E_g: 1.2–1.3 eV) [52], $Cu_2SbSe_3{\cdot}0.5en$ (E_g 1.58 eV), and $Cu_2SbSe_3{\cdot}en$ (E_g 1.61 eV) [53].

Conclusion

In summary, the ternary system Ln/Sb/Se (Ln=Sm, Eu, Gd, Ho) was investigated in tepa solvent under solvothermal conditions. Two types of Ln-tetraselenidoantimonate complexes with general formula $[[Ln(tepa)(Cl)][Ln(tepa)(OH)]_2(SbSe_4)_2]_n$ and $[H_2tepa][[Ln(tepa)(SbSe_4)]_2(OH)_2]$ have been prepared. The $[SbSe_4]^{3-}$ anion adopts μ-1κ:2κ-$SbSe_4$ and mono-$SbSe_4$ coordination modes in the

two types of Ln-tetraselenidoantimonate compounds, respectively. The coordination modes are different from those of the Ln-tetraselenidoantimonates, which were prepared in bidentate en and tridentate dien solvents. This observation shows synergetic effects of ethylene polyamines on the combination between Ln^{3+} and $[SbSe_4]^{3-}$ ions.

Experimental

All starting chemicals were of analytical grade and used as purchased. Elemental analyses were conducted using an MOD 1106 elemental analyzer. The micropobe analysis by energy dispersive X-ray spectroscopy (EDXS) was performed on a Hitachi S-4700 spectrometer. Fourier transform infrared (FT-IR) spectra were recorded with a Nicolet Magna-IR 550 spectrometer in dry KBr discs over the 4000–400 cm^{-1} range. Room-temperature optical diffuse reflectance spectra of the powder samples were obtained with a Shimadzu UV-3150 spectrometer. Absorption (α/S) data were calculated from the reflectance using the Kubelka–Munk function $\alpha/S = (1 - R^2)/2R$ [51], where R is the reflectance at a given energy, α is the absorption, and S is the scattering coefficient.

Tris(tetraethylenepentamine)bis(tetraselenidoantimonate)-dihydroxochlorotrisamarium(III)
(**1a**, $C_{24}H_{71}ClN_{15}O_2Sb_2Se_8Sm_3$)
$SmCl_3$ (128 mg, 0.5 mmol), 61 mg Sb (0.5 mmol), and 158 mg Se (2 mmol) were dispersed in 3 cm^3 of tepa by stirring, and the dispersion was loaded into a Teflon-lined stainless steel autoclave of 10 cm^3 volume. The reaction was run at 190 °C for 7 days. Upon cooling to ambient temperature, orange prism crystals of **1a** were filtered off, washed with ethanol, and stored under a vacuum (42 % yield based on Sb). Elemental analyses results of the crystals are consistent with the stoichiometry of $C_{24}H_{71}ClN_{15}O_2Sb_2Se_8Sm_3$. EDXS analysis gave the heavy atom component of $Sm_{3.21}Sb_{1.94}Se_{8.14}Cl$. IR (KBr): $\bar{\nu} = 3696$ (w), 3550 (m), 3426 (w), 3304 (w), 3130 (w), 2855 (w), 2202 (w), 1635 (w), 1589 (m), 1528 (m), 1435 (w), 1287 (s), 1131 (m), 1051 (m), 952 (s), 716 (m), 618 (m), 585 (m), 473 (w), 425 (w) cm^{-1}.

Tris(tetraethylenepentamine)bis(tetraselenidoantimonate)-dihydroxochlorotrieuropium (III)
(**1b**, $C_{24}H_{71}ClEu_3N_{15}O_2Sb_2Se_8$)
Orange block crystals of **1b** were obtained with a procedure similar to the synthesis of **1a**, except that $EuCl_3$ was used instead of $SmCl_3$ (45 % yield based on Sb). Elemental analysis results of the crystals are consistent with the stoichiometry of $C_{24}H_{71}ClEu_3N_{15}O_2Sb_2Se_8$. EDXS analysis gave the heavy atom component of $Eu_{3.13}Sb_{2.07}Se_{8.21}Cl$. IR (KBr): $\bar{\nu} = 3696$ (w), 3550 (m), 3304 (w), 3130 (w), 2947 (w), 2855 (w), 2202 (w), 1635 (w), 1589 (m), 1528 (m), 1435 (w), 1287 (s), 1131 (m), 1020 (m), 970 (s), 952 (s), 838 (m), 716 (m), 618 (m), 585 (m), 473 (w), 425 (w) cm^{-1}.

3,6,9-Triazaundecamethylenediammonium μ-dihydroxobis-[(tetraethylenepentamine)(tetraselenidoantimonate)-europate(III)] (**2a**, $C_{24}H_{73}Eu_2N_{15}O_2Sb_2Se_8$)
Orange block crystals of **2a** were obtained with a procedure similar to the synthesis of **1a**, except that Eu_2O_3 was used instead of $SmCl_3$ (44 % yield based on Sb). Elemental analysis results of the crystals are consistent with the stoichiometry of $C_{24}H_{73}Eu_2N_{15}O_2Sb_2Se_8$. EDXS analysis gave the heavy atom component of $EuSb_{2.11}Se_{4.12}$. IR (KBr): $\bar{\nu} = 3605$ (w), 3429 (m), 2929 (w), 2840 (w), 2360 (w), 1810 (w), 1721 (w), 1638 (m), 1571 (m), 1480 (m), 1423 (w), 1380 (w), 1304 (s), 1114 (m), 1051 (m), 913 (w), 854 (w), 810 (s), 713 (w), 592 (s), 493 (w), 406 (w) cm^{-1}.

3,6,9-Triazaundecamethylenediammonium μ-dihydroxobis-[(tetraethylenepentamine)(tetraselenidoantimonate)-gadolinate(III)] (**2b**, $C_{24}H_{73}Gd_2N_{15}O_2Sb_2Se_8$)
Yellow prism crystals of **2b** were obtained with a procedure similar to the synthesis of **1a**, except that Gd_2O_3 was used instead of $SmCl_3$ (48 % yield based on Sb). Elemental analysis results of the crystals are consistent with the stoichiometry of $C_{24}H_{73}Gd_2N_{15}O_2Sb_2Se_8$. EDXS analysis gave the heavy atom component of $GdSb_{1.98}Se_{4.05}$. IR (KBr): $\bar{\nu} = 3697$ (w), 3425 (s), 2945 (w), 2843 (w), 2083 (m), 1711 (w), 1639 (s), 1571 (w), 1495 (s), 1424 (m), 1380 (w), 1313 (s), 1190 (w), 1116 (m), 1050 (w), 958 (w), 889 (w), 807 (w), 761 (s), 692 (m), 592 (s), 492 (m), 419 (m) cm^{-1}.

3,6,9-Triazaundecamethylenediammonium μ-dihydroxobis-[(tetraethylenepentamine)(tetraselenidoantimonate)-holmate(III)] (**2c**, $C_{24}H_{73}Ho_2N_{15}O_2Sb_2Se_8$)
Yellow chip crystals of **2c** were obtained with a procedure similar to the synthesis of **1a**, except that Ho_2O_3 was used instead of $SmCl_3$ (49 % yield based on Sb). Elemental analysis results of the crystals are consistent with the stoichiometry of $C_{24}H_{73}Ho_2N_{15}O_2Sb_2Se_8$. EDXS analysis gave the heavy atom component of $HoSb_{2.15}Se_{4.09}$. IR (KBr): $\bar{\nu} = 3429$ (w), 3210 (m), 2946 (w), 2871 (w), 1571 (m), 1442 (m), 1361 (w), 1310 (w), 1260 (m), 1114 (m), 1080 (s), 1009 (m), 966 (m), 882 (m), 831 (w), 740 (w), 657 (s), 574 (m), 535 (s), 471 (m), 419 (w) cm^{-1}.

X-ray structure determination

Data were collected on a Rigaku Saturn (for **1a**, **1b**, **2b**, **2c**) or a Rigaku Mercury (for **2a**) CCD diffractometer, using graphite-monochromated Mo $K\alpha$ radiation ($\lambda = 0.71073$ Å)

Table 3 Crystallographic data and structure refinement details for **1a–2c**

	1a	**1b**	**2a**
Formula	$C_{24}H_{71}ClN_{15}O_2Sb_2Se_8Sm_3$	$C_{24}H_{71}ClEu_3N_{15}O_2Sb_2Se_8$	$C_{24}H_{73}Eu_2N_{15}O_2Sb_2Se_8$
Formula mass	1963.64	1968.47	1783.07
Dimensions/mm^3	0.30 × 0.25 × 0.10	0.30 × 0.25 × 0.18	0.50 × 0.20 × 0.10
Crystal system	Monoclinic	Monoclinic	Monoclinic
Space group	*C* 2/c	*C* 2/c	*C* 2/c
a/Å	29.372(3)	29.283(3)	28.250
b/Å	11.5496(8)	11.5536(10)	11.681(2)
c/Å	17.0842(14)	17.0705(17)	16.902(3)
β/°	97.504(2)	97.986(4)	108.26(3)
V/Å^3	5746.0(8)	5719.3(10)	5297.0(18)
Z	4	4	4
D_{calcd}/g cm^{-3}	2.270	2.286	2.258
F(000)	3652	3664	3392
μ/mm^{-1}	9.097	9.349	8.880
Max 2*θ*/°	50.70	50.70	50.70
Reflections collected	14,307	12,787	20,399
Independent reflections	5230	5195	4818
R_{int}	0.0374	0.0445	0.0682
Parameters	228	223	214
R_1 [$I > 2\sigma(I)$]	0.0379	0.0405	0.0336
wR_2 (all data)	0.0859	0.0982	0.0931
Goodness-of-fit on F^2	1.040	1.030	1.113

	2b	**2c**
Formula	$C_{24}H_{73}Gd_2N_{15}O_2Sb_2Se_8$	$C_{24}H_{73}Ho_2N_{15}O_2Sb_2Se_8$
Formula mass	1793.65	1809.01
Dimensions/mm^3	0.40 × 0.15 × 0.10	0.30 × 0.10 × 0.05
Crystal system	Monoclinic	Monoclinic
Space group	*C* 2/c	*C* 2/c
a/Å	28.134(4)	28.083(4)
b/Å	11.6208(13)	11.5786(14)
c/Å	16.861(2)	16.847(2)
β/°	108.777(3)	109.009(4)
V/Å^3	5219.0(12)	5179.4(12)
Z	4	4
D_{calcd}/g cm^{-3}	2.283	2.320
F(000)	3360	3384
μ/mm^{-1}	9.151	9.716
Max 2*θ*/°	50.70	50.70
Reflections collected	14,193	12,979
Independent reflections	4754	4720
R_{int}	0.0498	0.0748
Parameters	211	213
R_1 [$I > 2\sigma(I)$]	0.0346	0.0388
wR_2 (all data)	0.0956	0.0923
Goodness-of-fit on F^2	1.041	1.096

with a ω-scanning mode to a maximum 2θ value of 50.70°. An empirical absorption correction was applied for all compounds using the multi-scan method. All crystal structures were solved using SHELXS-97 [54], and refinement was performed against F^2 using SHELXL-97 [55]. All non-hydrogen atoms were refined anisotropically. Ln(2) and Cl(1) atoms in **1a** and **1b** are disordered, and the occupancies of both disordered atoms were refined as 50 and 50 %. The occupancies of the disordered atoms N(6) and N(7) of protonated H_2tepa cations in **1a** and **1b** were refined as 60 and 40 %, while the corresponding disordered atoms in **2c** were refined as 50 and 50 %. The hydrogen atoms were added geometrically and refined using the riding model. Crystallographic, experimental, and analytical data for the title compounds are listed in Table 3.

Crystallographic data for the structural analyses have been deposited with the Cambridge Crystallographic Data Center, CCDC Nos. 1057960, 1057961, 1057962, 1057963, and 1057964. These data can be obtained free of charge via https://summary.ccdc.cam.ac.uk/structure-summary-form.

Acknowledgments This work was supported by the National Natural Science Foundation of China (Grant No. 21171123), and the project funded by the Priority Academic Program Development (PAPD) of Jiangsu Higher Education Institutions.

References

1. Wachhold M, Kanatzidis MG (1999) Inorg Chem 38:3863
2. Wachhold M, Kanatzidis MG (2000) Inorg Chem 39:2337
3. Bera TK, Jang JI, Song J-H, Malliakas CD, Freeman AJ, Ketterson JB, Kanatzidis MG (2010) J Am Chem Soc 132:3484
4. Xiong WW, Athresh EU, Ng YT, Ding JF, Wu T, Zhang QC (2013) J Am Chem Soc 135:1256
5. Seidlhofer B, Spetzler V, Näther C, Bensch W (2012) J Solid State Chem 187:269
6. Schaefer M, Näther C, Lehnert N, Bensch W (2004) Inorg Chem 43:2914
7. Kiebach R, Pienack N, Ordolff ME, Studt F, Bensch W (2006) Chem Mater 18:1196
8. Liu GN, Guo GC, Chen F, Wang SH, Sun J, Huang JS (2012) Inorg Chem 51:472
9. Sheldrick WS, Wachhold M (1998) Coord Chem Rev 176:211
10. Li J, Chen Z, Wang RJ, Proserpio DM (1999) Coord Chem Rev 190–192:707
11. Sheldrick WS (2000) J Chem Soc Dalton Trans 3041
12. Seidlhofer B, Pienack N, Bensch W (2010) Z Naturforsch 65b:937
13. Zhou J, Dai J, Bian GQ, Li CY (2009) Coord Chem Rev 253:1221
14. Stephan HO, Kanatzidis MG (1996) J Am Chem Soc 118:12226
15. Vaqueiro P, Chippindale AM, Powell AV (2004) Inorg Chem 43:7963
16. Lees RJE, Powell AV, Chippindale AM (2005) Polyhedron 24:1941
17. Bensch W, Näther C, Stähler R (2001) Chem Commun 5:477
18. Stähler R, Bensch W (2002) Z Anorg Allg Chem 628:1657
19. Stähler R, Mosel BD, Eckert H, Bensch W (2002) Angew Chem Int Ed 41:4487
20. Yue CY, Lei XW, Ma YX, Sheng N, Yang YD, Liu GD, Zhai XR (2014) Cryst Growth Des 14:101
21. Stähler R, Näther C, Bensch W (2003) J Solid State Chem 174:264
22. Jin QY, Zhu AM, Pan YL, Jia DX, Zhang Y, Gu JS (2009) Z Anorg Allg Chem 635:139
23. Jia DX, Zhang Y, Zhao QX, Deng J (2006) Inorg Chem 45:9812
24. Schur M, Rijnberk H, Näther C, Bensch W (1999) Polyhedron 18:101
25. Schur M, Bensch W (2002) Z Naturforsch 57b:1
26. Engelke L, Stähler R, Schur M, Näther C, Bensch W, Pöttgen R, Möller MH (2004) Z Naturforsch 59b:869
27. Bensch W, Näther C, Schur M (1997) Chem Commun 18:1773
28. Almsick TV, Sheldrick WS (2006) Z Anorg Allg Chem 632:1413
29. Yue CY, Lei XW, Zang HP, Zhai XR, Feng LJ, Zhao ZF, Zhao JQ, Liu XY (2014) CrystEngComm 16:3424
30. Möller K, Näther C, Bannwarth A, Bensch W (2007) Z Anorg Allg Chem 633:2635
31. Stähler R, Bensch W (2001) Eur J Inorg Chem 3073
32. Schaefer M, Kurowski D, Pfitzner A, Näther C, Rejai Z, Möller K, Ziegler N, Bensch W (2006) Inorg Chem 45:3726
33. Schaefer M, Stähler R, Kiebach WR, Näther C, Bensch W (2004) Z Anorg Allg Chem 630:1816
34. Schaefer M, Näther C, Bensch W (2004) Monatsh Chem 135:461
35. Stähler R, Bensch W (2001) J Chem Soc Dalton Trans 2518
36. Schaefer M, Engelke L, Bensch W (2003) Z Anorg Allg Chem 629:1912
37. Lichte J, Lühmann H, Näther C, Bensch W (2009) Z Anorg Allg Chem 635:2021
38. Nie L, Xiong WW, Li PZ, Han JY, Zhang GD, Yin SM, Zhao YL, Xu R, Zhang QC (2014) J Solid State Chem 220:118
39. Pan YL, Chen JF, Wang J, Zhang Y, Jia DX (2010) Inorg Chem Commun 13:1569
40. Tang WW, Chen RH, Zhao J, Jiang WQ, Zhang Y, Jia DX (2012) CrystEngComm 14:5021
41. Jia DX, Jin QY, Chen JF, Pan YL, Zhang Y (2009) Inorg Chem 48:8286
42. Chen RH, Tang WW, Jiang WQ, Zhang Y, Jia DX (2013) J Coord Chem 66:650
43. Jia DX, Zhu AM, Jin QY, Zhang Y, Jiang WQ (2008) J Solid State Chem 181:2370
44. Zhao J, Liang JJ, Pan YL, Zhang Y, Jia DX (2011) J Solid State Chem 184:1451
45. Cassol A, Bernardo PDi, Portanova R, Tolazzi M, Tomat G, Zanonato P (1992) J Chem Soc Dalton Trans 469
46. Zhou J, An LT, Hu FL, Liu X, Zhao RQ, Lin JW (2012) CrystEngComm 14:5544
47. Zhou J, Hu FL, An LT, Liu X, Meng CY (2012) Dalton Trans 41:11760
48. Xiao HP, Zhou J, Zhao RQ, Zhang WB, Huang Y (2015) Dalton Trans 44:6032
49. Liu Y, Tang CY, Han JY, Shen YL, Lu JL, Jia DX (2015) Inorg Chem Commun 60:103
50. Jin QY, Chen JF, Pan YL, Zhang Y, Jia DX (2010) J Coord Chem 63:1492
51. Wendlandt WW, Hecht HG (1966) Reflectance spectroscopy. Interscience Publishers, New York
52. Chen Z, Wang RJ, Dilks KJ, Li J (1999) J Solid State Chem 147:132
53. Chen Z, Dilks RE, Wang RJ, Lu JY, Li J (1998) Chem Mater 10:3184
54. Sheldrick GM (1997) SHELXS-97 program for solution of crystal structures. University of Göttingen, Germany
55. Sheldrick GM (1997) SHELXL-97 program for refinement of crystal structures. University of Göttingen, Germany